Controlling Two-Center Interference in Molecular High Harmonic Generation

C. Vozzi, F. Calegari, E. Benedetti, J.-P. Caumes, G. Sansone, S. Stagira, and M. Nisoli
Dipartimento di Fisica, Politecnico, National Laboratory for Ultrafast and Ultraintense Optical Science—CNR-INFM, Milano, Italy

R. Torres, E. Heesel, N. Kajumba, and J. P. Marangos*
The Blackett Laboratory, Imperial College London, Prince Consort Road, London SW7 2BW, United Kingdom

C. Altucci and R. Velotta
CNISM and Dipartimento di Scienze Fisiche, Università di Napoli "Federico II", Napoli, Italy
(Received 24 May 2005; published 4 October 2005)

We experimentally investigate the process of intramolecular quantum interference in high-order harmonic generation in impulsively aligned CO_2 molecules. The recombination interference effect is clearly seen through the order dependence of the harmonic yield in an aligned sample. The experimental results can be well modeled assuming that the effective de Broglie wavelength of the returning electron wave is not significantly altered by the Coulomb field of the molecular ion. We demonstrate that such interference effects can be effectively controlled by changing the ellipticity of the driving laser field.

DOI: 10.1103/PhysRevLett.95.153902 PACS numbers: 42.65.Ky, 42.65.Re

The investigation of high-order harmonic generation (HHG) [1–3] in aligned ensembles of molecules [4] has recently emerged as an important area in strong field ultrafast physics. This is because it may be possible to use the molecular alignment to control harmonic emission [5] and potentially enhance attosecond pulse generation [6]. It has been shown that the dependence of HHG on the molecular structure [7] can give new ways of measuring molecular structure. The recent demonstration of tomographic reconstruction of the electronic state of the N_2 molecule was a first step in implementing these ideas of imaging [3].

HHG in the strong field limit can be seen as a three step process [8,9]: (i) tunnel ionization of the most weakly bound electron near the peak of the laser cycle; (ii) acceleration in the time varying laser field; (iii) recombination of the continuum electron [described approximately by a plane wave, $\psi_c \sim \exp(-i\mathbf{kr})$] into the bound electronic state. A unique aspect of HHG in a simple molecular system is the possibility of observing quantum interference phenomena between the contributions from different parts of the extended molecular wave function. Numerical simulations of the HHG process from H_2^+ and H_2 as a function of the angle θ between the laser polarization and the internuclear axis showed interference in the recombination step of the HHG process between the dipole amplitudes from the two atomic centers in the molecule, when they were separated by half a de Broglie wavelength λ_B [7,10]. Recently this effect was observed in aligned CO_2 molecules by Kanai *et al.* [11].

We analyze the role of two-center interference in aligned CO_2 molecules by measuring the harmonic spectrum up to the 49th (76 eV) order revealing the full shape of the destructive interference modulation. This is well fitted by a simple model for the interference process that confirms that the effective value of λ_B of the returning continuum electron is the usual value in the absence of a Coulomb field. For the first time, to our knowledge, we demonstrate that such interference effects can be controlled by changing the polarization state of the driving laser field.

In these experiments the molecular alignment is controlled by an initial ultrafast laser pulse, that excites a *rotational wave packet* (coherent superposition of rotational states) in the molecule [12,13]. The rotational wave packet exhibits strong molecular axis alignment at a regular period corresponding to rotational revivals, half-revivals, and quarter revivals, with a field free alignment at the rotational revivals and subrevivals. A delayed higher intensity ultrafast laser pulse produces high harmonic emission from the molecules when they are close to the maximum degree of alignment. By varying the precise delay of this pulse the HHG emission intensity for different magnitudes and angles of alignment can be measured.

In our experimental configuration, the light pulses generated by a Ti:Sapphire laser system with chirped pulse amplification were split into two beams, which were separately amplified up to 1 mJ, by means of further amplification stages and separately compressed. The pump (aligning pulse) and probe (driving pulse for the harmonic generation) pulses were then collinearly focused with a variable mutual delay on a pulsed supersonic molecular jet in the interaction chamber. The focus of the laser was around 3 nozzle diameters below the orifice, leading to a rotational temperature of a few tens of K. With this configuration, the aligning pulse had an energy of $\sim$200 μJ and a duration of $\sim$60 fs; the linear polarization of the aligning beam was controlled by means of a half-wave plate. The energy of the 30 fs probe pulse was $\sim$250 μJ, and its polarization state was changed from linear to circular with a quarter-wave plate. Generated harmonics were dispersed and detected by a high-resolution flat-field spectrometer and a high-resolution CCD detector [14].

Figures 1(a) and 1(b) show the evolution of the photon yield of the 33rd and 49th harmonics, respectively, measured in CO_2 as a function of pump-probe delay, with parallel polarization of the two pulses. The photon yield has been normalized to that measured in the gas without alignment beam. The photon yield is significantly modulated with a period given by the rotational period, T_r, of CO_2 ($T_r = 42.8$ ps). Figures 1(a) and 1(b) show the first half-revival (pump-probe delay $\tau \sim 21.4$ ps). The calculated evolution of $\langle\cos^2\theta\rangle$ is also displayed in Figs. 1(a) and 1(b), with the full weighted distribution function for several times near the peak of the revival shown in Fig. 1(c) [13]. The evolution of the yield of the two harmonics is completely different. While the photon yield of the 33rd harmonic presents a temporal evolution inverted with respect to that of $\langle\cos^2\theta\rangle$, in agreement with the results reported by Kanai *et al.* [11], the photon yield of the 49th harmonic presents a different modulation.

We then fixed the pump-probe delay, τ, in correspondence to the maximum of $\langle\cos^2\theta\rangle$, around the position of the first half-revival [$\tau = 21.1$ ps; this delay is indicated by the letter A in Fig. 1(a)], and measured the harmonic spectra with and without the pump beam (pump and probe pulses with parallel polarization). The results are shown in Fig. 2(a): a pronounced depression of the harmonic generation is visible around the 33rd order in the aligned case. In order to analyze the effect, we have extracted the integrated intensity, Φ, for each harmonic order. The solid line in Fig. 2(b) shows the ratio Φ/Φ_0, between the harmonic intensities measured with (Φ) and without (Φ_0) the aligning pulse. A clear and broad minimum around the position of the 33rd harmonic is evident with $\Phi/\Phi_0 < 1$. This is consistent with the behavior reported by Kanai *et al.* [11], although in our measurements the minimum is shifted several harmonic orders higher. Beyond the minimum the ratio then increases with harmonic order and becomes larger than unity at high photon energy (49th harmonic).

As shown by Kanai *et al.* [11], the measured inversion of the temporal evolution of the revival structure with respect to that of $\langle\cos^2\theta\rangle$ [shown in Fig. 1(a)] can be explained in terms of destructive quantum interference in the recombi-

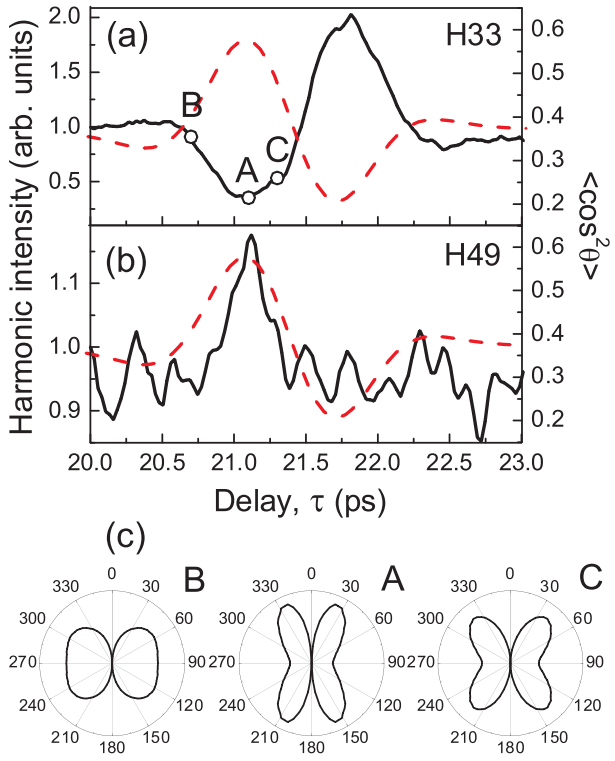

FIG. 1 (color online). Modulation of the harmonic yield in impulsively aligned CO_2 molecules due to half-revival of rotational wave packet (a) for the 33rd and (b) 49th harmonic order. Pump and probe pulses with parallel polarization. Pump pulse: energy 200 μJ, duration 60 fs. Probe pulse: intensity 2×10^{14} W/cm^2, duration 30 fs. Dashed curve in (a) and (b) displays the calculated temporal evolution of the corresponding $\langle\cos^2\theta\rangle$. (c) Polar plot of the θ distribution for different pump-probe delays: $\tau = 20.7$, 21.1, and 21.3 ps.

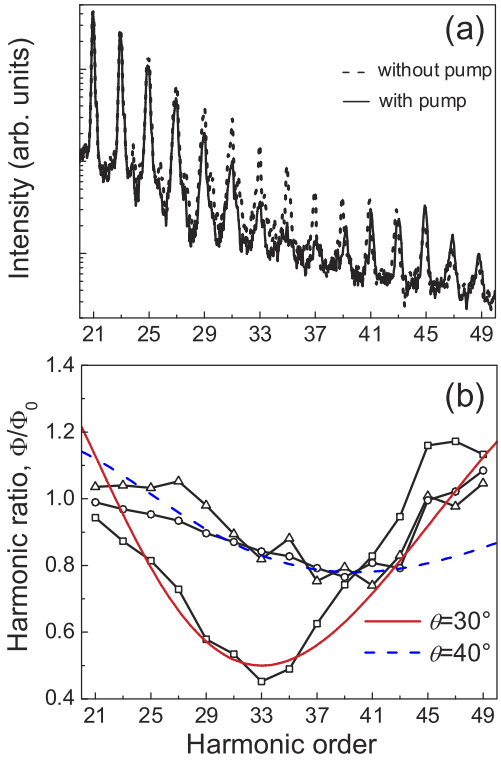

FIG. 2 (color online). (a) Measured harmonic spectra generated by 30 fs pulses with (solid curve) and without (dashed curve) pump beam (pump and probe pulses with parallel polarization). Pump-probe delay $\tau = 21.1$ ps. (b) Ratio Φ/Φ_0, between the harmonic intensities measured with (Φ) and without (Φ_0) the pump pulse, measured at three pump-probe delays: $\tau = 20.7$ ps (circles), 21.1 ps (squares), and 21.3 ps (triangles). The lines show the modulation in harmonic yield predicted by Eq. (1) (with a vertical offset term added) for $\theta = 30°$ [solid (red online) curve] and $\theta = 40°$ [dashed (blue online) curve].

nation step. This interpretation is additionally supported by our observation of revival reversal at larger harmonic orders, e.g., 49th, as displayed in Fig. 1(b). In fact, outside the region of destructive interference the harmonic yield is dominated by the ionization rate of the medium, and maximizes at the same pump-probe delays as $\langle\cos^2\theta\rangle$ [11], which corresponds to when the molecules are aligned at $\theta \approx 30°$.

As pointed out in Ref. [7], the interference pattern can be predicted by a simple physical argument which treats the nuclei as point emitters. The CO_2 molecule can be considered as a two-center molecule, with the corresponding point emitters placed on the two oxygen atoms. In this simple approach the harmonic yield is modulated as

$$I(n, \theta) = I_0(\theta)\left[1 \pm \cos\left(\frac{2\pi R\cos\theta}{\lambda_B(n)}\right)\right] \qquad (1)$$

where the sign $\pm$ refers to symmetric and antisymmetric orbitals, respectively (CO_2 has an antisymmetric orbital); moreover, θ is the angle between laser polarization and the internuclear axis; R is the internuclear separation (distance between the two O atoms in the CO_2 molecule: $R = 0.232$ nm); $\lambda_B(n)$ is the de Broglie wavelength of an electron responsible for the emission of the nth harmonic, given here by $\lambda_B(n) = h/\sqrt{2m_e(nh\nu_0 - I_P)}$, where m_e is the electron mass; $nh\nu_0$ is the emitted photon energy ($h\nu_0 = 1.55$ eV); and I_P is the ionization potential ($I_P = 13.77$ eV). Using Eq. (1), the angle θ corresponding to the condition of destructive interference around the 33rd harmonic order is $\sim 30°$. This is in excellent agreement with the calculated θ distribution, shown in Fig. 1(c) for three pump-probe delays (corresponding to the points marked as A, B, and C in Fig. 1(a)]. Corresponding to the maximum of the $\langle\cos^2\theta\rangle$ curve, point A (delay $\tau = 21.1$ ps), the θ distribution shows a "butterfly" structure, with a modal value for the molecular axis of $\theta \sim 30°$. The spectral window where a significant decrease of the harmonic yield is observed is rather large, in agreement with the simulations reported in [7]. Considering pump-probe delays located on opposite sides of the maximum of the $\langle\cos^2\theta\rangle$ curve, points B and C in Fig. 1(a), the θ distribution still shows a butterfly structure, but with a modal value increased to $\theta \sim 40°$. In these cases, the harmonic order corresponding to the condition for destructive interference predicted by Eq. (1) should increase. This effect is clearly shown by the experimental curves in Fig. 2(b), which display the harmonic ratio Φ/Φ_0 measured at the pump-probe delays corresponding to the points B and C of Fig. 1(a) ($\tau = 20.7$ ps and $\tau = 21.3$ ps): the minimum is reached around the 39th harmonic order.

The whole behavior of Φ/Φ_0 ratio as a function of the harmonic order is well reproduced by Eq. (1) (with a vertical offset added) which is plotted in Fig. 2(b) for $\theta = 30°$ [solid (red online) curve] and $\theta = 40°$ [dashed (blue online) curve]. In particular the position of the minima predicted by this simple model are in close agreement with the measured data. This strongly supports the conclusion that the effective electron wavelength in the recollision with the molecule is $\lambda_B(n) = h/\sqrt{2m_e(nh\nu_0 - I_P)}$, i.e., the value expected for a continuum electron in the absence of the Coulomb field. This result may be explained by the fact that the molecular electronic state is spatially extended so that the matrix element for the recombination step is dominated by regions outside of the strong influence of the core.

In order to further explore the role of intramolecular interference, we have measured the dependence of harmonic generation upon ellipticity of the probe beam. For this purpose a zero-order quarter wave plate was placed in the linearly polarized probe beam. It is well known that the harmonic generation process is very sensitive to the polarization of the driving pulses; the efficiency rapidly decreases upon increasing the ellipticity ϵ [15]. Figure 3 shows the ellipticity dependence of the photon yield of three harmonics (23rd, 33rd, and 47th) in the case of aligned (solid curves) and randomly oriented (dashed curves) molecules, measured at a pump-probe delay $\tau = 21.1$ ps. It is evident that around the 33rd harmonic, i.e., for the harmonic orders corresponding to the destructive interference minimum, dramatic differences in the ellipticity

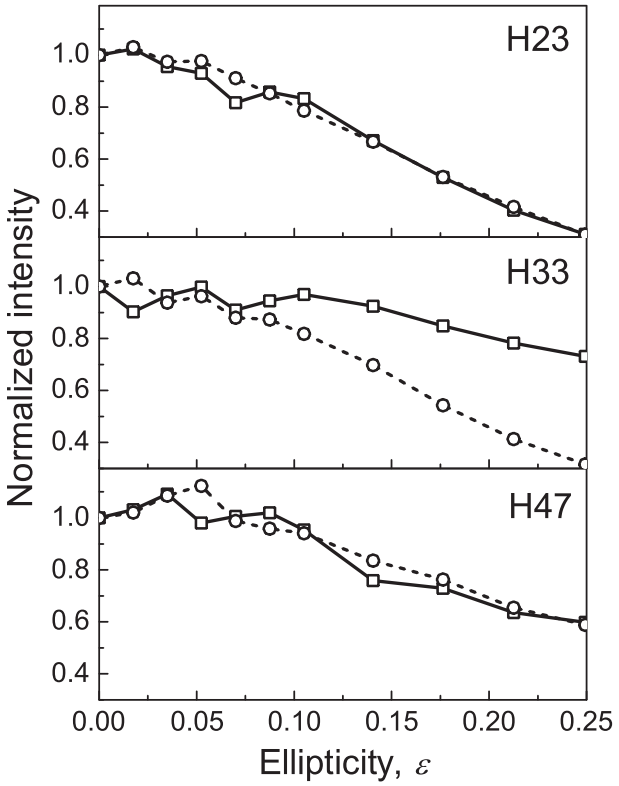

FIG. 3. Ellipticity dependence of the harmonic yield for three different harmonic orders measured in aligned (solid curve) and not aligned (dashed curve) normalized to the zero ellipticity case. Pump-probe delay $\tau = 21.1$ ps.

dependence are measured in aligned and unaligned molecules. For the orders where destructive interference is strong, the HHG signal is much less influenced by ellipticity in the aligned sample compared to the unaligned sample. The harmonic yield of the 33rd order barely drops up to values of $\epsilon > 0.25$. For the harmonic orders not strongly affected by destructive interference (below the 25th and above the 47th) there are only slight differences between the aligned and unaligned case.

A simple interpretation of these experimental results can be given in the framework of the intramolecular two-center interference. Even if the simple condition for destructive interference given by Eq. (1) cannot be directly applied in the case of elliptical polarization, the physical interpretation of the interference effect is still valid. In fact, the relevant angle for the interference is that formed by the electron wave vector and the molecular axis, which coincides with θ in Eq. (1) when linearly polarized light is considered. We have calculated the electron motion in the continuum in the presence of an elliptically polarized laser field [15]. In this way we have obtained the tilt of the electron wave vector with respect to θ in terms of the ratio between the two velocity components of the recolliding electron at the instant of recombination with the parent ion. For low ellipticity values it turns out that the variation of electron direction with respect to the linearly polarized case is smaller than the spreading of the molecular angular distribution [see polar plot A in Fig. 1(c)], making the destructive interference still observable. This is no longer valid for larger ellipticity values. In summary, for low ϵ values the harmonic emission from aligned molecules is significantly reduced by the intramolecular interference, while at larger ellipticity values destructive interference plays a minor role and the ellipticity dependence will be more influenced by the increased ionization of the aligned molecules. These results show how the two-center interference can be controlled through the control of laser ellipticity. Effectively the interference can be switched off and then only the effects of the first step of the harmonic generation process (ionization) will determine the yield. This may have application to controlling HHG yield, but also points to a broader class of applications in the steering of strong field molecular processes through ellipticity and alignment angle control.

In conclusion, we have measured the modulation of harmonic signal due to the rotational revival structure in impulsively aligned CO_2 molecules. The role of two-center quantum interference in the electron recombination step has been analyzed. We have shown that the de Broglie wavelength of the continuum electron in this process is that in a constant potential without significant influence from the Coulomb field. Very anomalous ellipticity dependence is measured under these conditions, with the harmonic signal remaining almost constant even when the ellipticity is increased to $\epsilon = 0.25$, as a consequence of the recombination being tuned away from the destructive interference condition by the changed field ellipticity, while the ionization rate remains high.

We acknowledge the support of the European Community under ''Laserlab-Europe'' Integrated Infrastructure Initiative Contract No. RII3-CT-2003-506350 and Project No. MRTN-CT-2003-505138 (XTRA). The authors gratefully acknowledge the contribution of L. Poletto and P. Villoresi for the development of the XUV spectrometer. R. T. acknowledges the Spanish Ministry of Education for financial support.

*Corresponding author.
Email address: j.marangos@imperial.ac.uk

[1] R. Velotta, N. Hay, M. B. Mason, M. Castillejo, and J. P. Marangos, Phys. Rev. Lett. **87**, 183901 (2001).
[2] M. Kaku, K. Masuda, and K. Miyazaki, Jpn. J. Appl. Phys. **43**, L591 (2004).
[3] J. Itatani, J. Levesque, D. Zeidler, H. Niikura, H. Pepin, J. C. Kieffer, P. B. Corkum, and D. M. Villeneuve, Nature (London) **432**, 867 (2004).
[4] H. Stapelfeldt and T. Seidemann, Rev. Mod. Phys. **75**, 543 (2003).
[5] J. Itatani, D. Zeidler, J. Levesque, M. Spanner, D. M. Villeneuve, and P. B. Corkum, Phys. Rev. Lett. **94**, 123902 (2005).
[6] T. Pfeifer, D. Walter, and G. Gerber, M. Yu. Emelin, M. Yu. Ryabikin, M. D. Chernobrovtseva, and A. M. Sergeev, Phys. Rev. A **70**, 013805 (2004).
[7] M. Lein, N. Hay, R. Velotta, J. P. Marangos, and P. L. Knight, Phys. Rev. A **66**, 023805 (2002).
[8] P. B. Corkum, Phys. Rev. Lett. **71**, 1994 (1993).
[9] K. C. Kulander, K. J. Schafer, and J. L. Krause, in *Proceedings of the Workshop, Super Intense Laser Atom Physics (SILAP) III*, edited by B. Piraux (Plenum Press, New York, 1994).
[10] M. Lein, N. Hay, R. Velotta, J. P. Marangos, and P. L. Knight, Phys. Rev. Lett. **88**, 183903 (2002).
[11] T. Kanai, S. Minemoto, and H. Sakai, Nature (London) **435**, 470 (2005).
[12] F. Rosca-Pruna and M. J. J. Vrakking, J. Chem. Phys. **116**, 6567 (2002).
[13] R. Torres, R. de Nalda, and J. P. Marangos, Phys. Rev. A **72**, 023420 (2005).
[14] L. Poletto, S. Bonora, M. Pascolini, and P. Villoresi, Rev. Sci. Instrum. **75**, 4413 (2004).
[15] P. Dietrich, N. H. Burnett, M. Ivanov, and P. B. Corkum, Phys. Rev. A **50**, R3585 (1994).